COMPUTATIONAL SCIENCE&DISCOVERY

Artificial crawler model for texture analysis on silk fibroin scaffolds

Bruno Brandoli Machado[1,2]**, Wesley Nunes Gonçalves**[1,3] **and Odemir Martinez Bruno**[2,3]

[1] Federal University of Mato Grosso do Sul, University of São Paulo (USP), Avenida Trabalhador São-Carlense, 400, 13560-970 São Carlos, SP, Brazil
[2] Institute of Mathematical Sciences and Computing (ICMC), University of São Paulo (USP), Avenida Trabalhador São-Carlense, 400, 13560-970 São Carlos, SP, Brazil
[3] Physics Institute of São Carlos (IFSC), University of São Paulo (USP), Avenida Trabalhador São-Carlense, 400, 13560-970 São Carlos, SP, Brazil
E-mail: brandoli@icmc.usp.br, wnunes@ursa.ifsc.usp.br and bruno@ifsc.usp.br

Abstract. Texture plays an important role in computer vision tasks. Several methods of texture analysis are available. However, these methods are not capable of extracting rich detail in images. This paper presents a novel approach to image texture classification based on the artificial crawler model. Here, we propose a new rule of movement that moves artificial crawler agents not only toward higher intensities but also toward lower ones. This strategy is able of capturing more detail because the agents explore the peaks as well as the valleys. Thus, compared with the state-of-the-art method, this approach shows an increased discriminatory power. Experiments on the most well known benchmark demonstrate the superior performance of our approach. We also tested our approach on silk fibroin scaffold analysis, and results indicate that our method is consistent and can be applied in real-world situations.

Q1

Contents

1. Introduction

Numerous approaches have been developed for texture analysis in different domains such as image analysis, quality inspection [1], plant species analysis [2], remote sensing [3] and medical image analysis [4]. Typically, these methods are based on *statistical analysis* of the spatial distribution (e.g. co-occurrence matrices [5] and local binary pattern [6]), *stochastic models* (e.g. Markov random fields [7]), *spectral analysis* (e.g. Fourier descriptors [8], Gabor filters [9, 10] and wavelet transforms [11]), *complexity analysis* (e.g. fractal dimension [12, 13]), *agent-based model* (e.g. deterministic tourist walk [14, 15]). Despite the existence of several texture methods, none can effectively capture the richness of patterns of silk fibroin scaffolds.

Silk fibroin is extracted from the cocoons of the silkworm Bombyx mori. It has recently been used as a protein biomaterial for the formation of scaffolds for a number of applications of biomedical sciences due to its high capacity to regenerate bones and tissues. In addition, it also has good mechanical properties in terms of flexibility for growth and adhesion in human prosthesis [16, 17]. Such properties have motivated researchers to investigate different silk fibroin scaffolds by adding glycerol [17]. However, they have not been able to determine the exact amount of glycerol needed because the mix can alter the interactions among the silk fibroin molecules, damaging the result on its surface. Therefore, texture analysis methodology has emerged as a framework for testing the suitable concentration of glycerol.

This paper presents a methodology for classifying surface properties of silk fibroin scaffolds using texture analysis. The approach proposed here is based on the artificial crawler model [18–20]. We propose a new rule of movement that moves artificial crawler agents not only toward higher intensities but also toward lower ones. We confirm that this strategy increases the discriminatory power and overcomes the limitations of the traditional methodology as well as the state-of-the-art method.

This paper is organized as follows. Section 2 describes the original artificial crawler model in detail. The proposed approach for characterizing texture images is presented in section 3. Section 4 discusses the experimental setup for and the results of two experiments. Computational complexity is discussed in section 5. Finally, conclusions are given in section 6.

2. The original artificial Crawler model

The original texture description approach was developed by Zhang and Chen [18, 19]. Zhang and Chen referred to their model as the artificial crawler (ACrawler) model. Given an image as a pair (Υ, I), consisting of a finite set Υ of pixels, and a mapping I that assigns to each pixel $p = (x_p, y_p) \in \Upsilon$ an intensity $I(p)$ ranging from 0 to 255. A pixel of the intensity map I holds a neighborhood set $\eta(p)$ of pixels q, where $d(p, q) \leqslant \sqrt{2}$ is the Euclidean distance between pixels p and q. Therefore, we assume there are eight connected neighbors

Q2

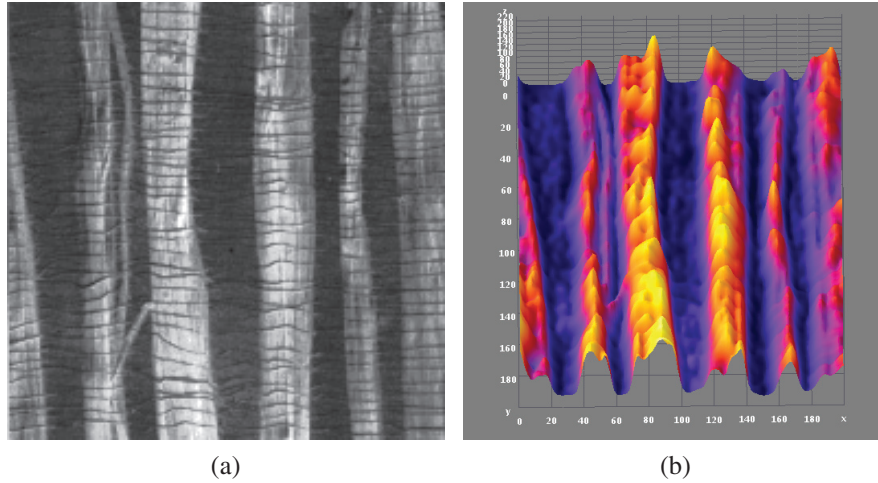$$d(p, q) = \sqrt{(x_p - x_q)^2 + (y_p - y_q)^2}. \tag{1}$$

Figure 1. The environment of the agents. On the left is shown a textured image (a) and its respective 3D surface (b).

The original model assumes that each live agent represents one pixel of the image. At each time t, an agent i is characterized by two attributes: its energy level e_i^t and its position in the image ρ_i^t. First, n agents are born with identical energy ϵ. Such energy can either wax or wane during their lifespan according to energy consumption and influence of the environment. In images, the environment is treated as a three-dimensional (3D) surface with different altitudes that correspond to gray values on the z-axis of the images. Higher intensities supply nutrients to the agents, while lower altitudes correspond to the land. Figure 1 shows a textured image and the peaks and valleys where the agents can live.

The algorithm consists of a set of rules that comprises the evolution process:

1. *Born.* Each agent i is born with the same energy ϵ

$$\forall_i \quad e_i^0 = \epsilon.$$

2. *Survival threshold.* An agent i dies if its energy is below the threshold:

$$\forall_{t,i} \quad \text{if } e_i^t \leqslant e_{\min} \text{ then } i \text{ dies.}$$

3. *Movement.*

$$\forall_i \quad e_i^t > e_{\min}, \rho_i^{t+1} = f(\rho_i^t).$$

$$f(\rho) = \begin{cases} \rho_i^t & \text{if (a) is satisfied,} \\ \rho_{\max}^t & \text{if (b) is satisfied,} \\ \rho_m^t & \text{if (c) is satisfied.} \end{cases}$$

   (a) Agents settle down if the gray level of its eight neighbors is lower than itself.
   (b) Agents move to a specific pixel if one of its eight neighbors ($\rho_{\max}^t$) has higher intensity.
   (c) If there is more than one neighbor with higher intensity, an agent moves to the pixel that was already occupied by another agent (ρ_m^t).

4. *Energy consumption.* Each time, t consumes a certain amount of energy, usually set to $e_{\text{unit}} = 1$:

$$\forall_i \quad e_i^t > e_{\min}, e_i^{t+1} = e_i^t - e_{\text{unity}}.$$

5. *Law of the jungle.* An agent with higher energy eats up another with lower energy

$$\forall_{i,j} \quad \rho_i^{t+1} = \rho_j^{t+1}, e_{\max}\{e_i^t, e_j^t\} = \max\{e_i^t, e_j^t\}.$$

3

6. *Gain of energy*. Each agent absorbs some energy from its environment at a rate of λ, according to

$$\forall_i \quad e_i^{t+1} = e_i^t + \lambda I(\rho_i^t).$$

7. *Limit of energy*. The energy is bound from above, according to

$$\forall_{t,j} \quad e_j^t \geqslant e_{\max}, e_j^{t+1} = e_{\max}.$$

Agents that were born in lower altitude regions absorb less energy and tend to die in the evolution process. On the other hand, agents that reached regions of higher altitudes have higher energy, thus a higher likelihood of remaining alive. The law of the jungle (rule 5) is inspired by nature and assumes that the agents with higher energy are more likely to reach the peaks of the environment.

To quantify the multi-agent system, a curve of live agents at each time is obtained:

$$\varphi = [\psi(0), \psi(1), \ldots, \psi(t_{\max})], \tag{2}$$

where $\psi(t)$ is the number of live agents at time t and $t_{\max}$ is the maximum iteration.

3. A novel approach to texture analysis with the artificial Crawler model

The original artificial crawler model consists of moving a group of agents to a neighboring pixel toward the highest intensity. Although images have been characterized using this model, the it does not display the full richness of the textural pattern. Our approach differs from the original ACrawler model in terms of movement: each agent is able to move not only to higher altitudes but also to lower ones. This allows the model to render the detail present in both peaks and valleys of the images.

First, the agents move to higher intensities as in the original artificial crawler method. Thus, artificial crawlers are performed using this rule and the curve $\varphi_{\max}$ is obtained. Throughout the paper, this rule of movement will be referred to as max. We observe that the original artificial crawler method models only the peaks of a textured image. To obtain a robust and effective texture representation, we propose moving artificial crawlers toward lower intensities as well. This rule of movement will be referred to throughout the paper as min. In our approach, artificial crawlers are randomly placed in the image with initial energy ϵ. Then, the movement step is modified as follows:

$$\forall_i \quad e_i^t > e_{\min}, \rho_i^{t+1} = f(\rho_i^t),$$

$$f(\rho) = \begin{cases} \rho_i^t & \text{if (a) is satisfied,} \\ \rho_{\min}^t & \text{if (b) is satisfied,} \\ \rho_m^t & \text{if (c) is satisfied.} \end{cases}$$

(a) Agents settle down if the gray level of their eight neighbors is higher than their own.

(b) Agents move to a specific pixel if there one of its eight neighbors ($\rho_{\min}^t$) has lower intensity

(c) If there is more than one neighbor with lower intensity, an agent moves to the pixel that was already occupied (ρ_m^t).

The multi-agent system using the rule of movement min is characterized as the original method by using the number of live agents at each time. Considering that we now have two rules of movement, the final feature vector of our approach is composed by the concatenation of $\varphi_{\max}$ and $\varphi_{\min}$ according to equation (2):

$$\varphi = [\varphi_{\max}, \varphi_{\min}]. \tag{3}$$

In order to obtain the final feature vector we run our approach for the maximum intensity as well as the minimum one. Despite the fact that this strategy doubles the computing time, it allows us to extract the details present in the peaks and valleys of images.

Figure 2 shows the curves of the evolution process. We took two classes of textures (on the top right-hand corner in figure 2) from the album Brodatz [21] to illustrate the separability. On the left, figure 2 shows the number of live agents using the rule of movement min, while the curve for the rule of movement max is shown on the right side of figure 2. The experimental results below corroborate the importance of both rules of movement in the texture modeling.
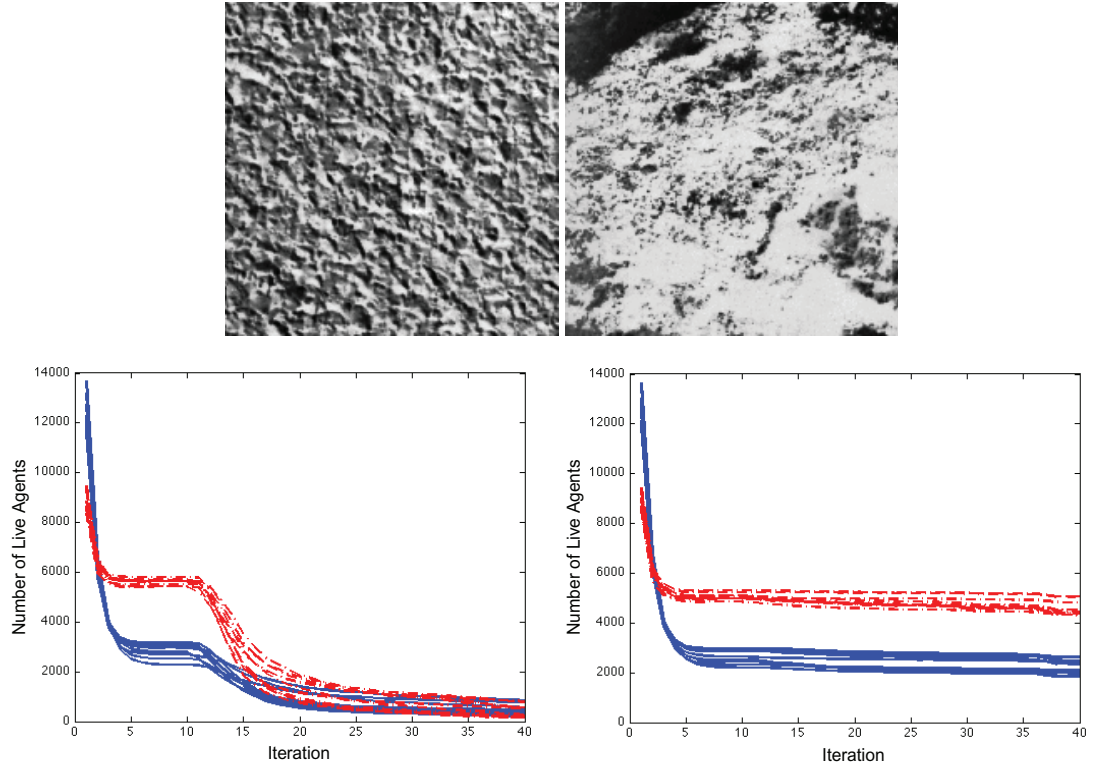
Figure 2. Curve of live agents using the rules of movement max (left) and min(right).

4. Experimental results

In this section, we demonstrate the effectiveness of our approach. We first outline the details of the experimental setup, then describe the experiments carried out on two datasets: Brodatz and silk fibroin. In section 4.2 we describe the whole process for image acquisition of silk fibroin scaffolds. In addition, we compare our results with those of different texture methods.

4.1. Experimental setup

The proposed method was first evaluated in texture classification experiments by using images extracted from the Brodatz album [21]. This album is considered a well-known benchmark for evaluating texture recognition methods. Each class is composed of one image divided into nine non-overlapping sub-images. A total of 440 images grouped into 40 classes was considered. Each image is 200×200 pixels in size and has 256 gray levels. One example of each class is shown in figure 3.

      The texture classification was carried out for ten-fold cross validation to avoid bias. At each round, we randomly divide the samples of each class into ten subsets of the same size, i.e. nine for training and the remaining for testing. The results are reported as the average value over the ten runs. For classification, we adopted the model linear discriminant analysis (LDA). The underlying idea is to maximize the Euclidian distance between the means of the classes while minimizing the within-class variance. For further information we refer to [22].

      LDA [23] was selected since it is well founded in statistical learning theory and has been successfully applied to various object detection tasks in computer vision. LDA, originally proposed by Fisher, computes a linear transformation ($T \in \Re^{d \times n}$) of D, which $D \in \Re^{d \times n}$ is a matrix and d denotes the number of features and n number of samples.

      We optimized two parameters of the artificial crawler model: the number of agents and the way that agents move in the evolution process. The number of agents placed on the pixels of the image was initial set to 1000 with a coverage rate of 10%, varying from 1000 to 35 000. In our experiments, all agents were born with an
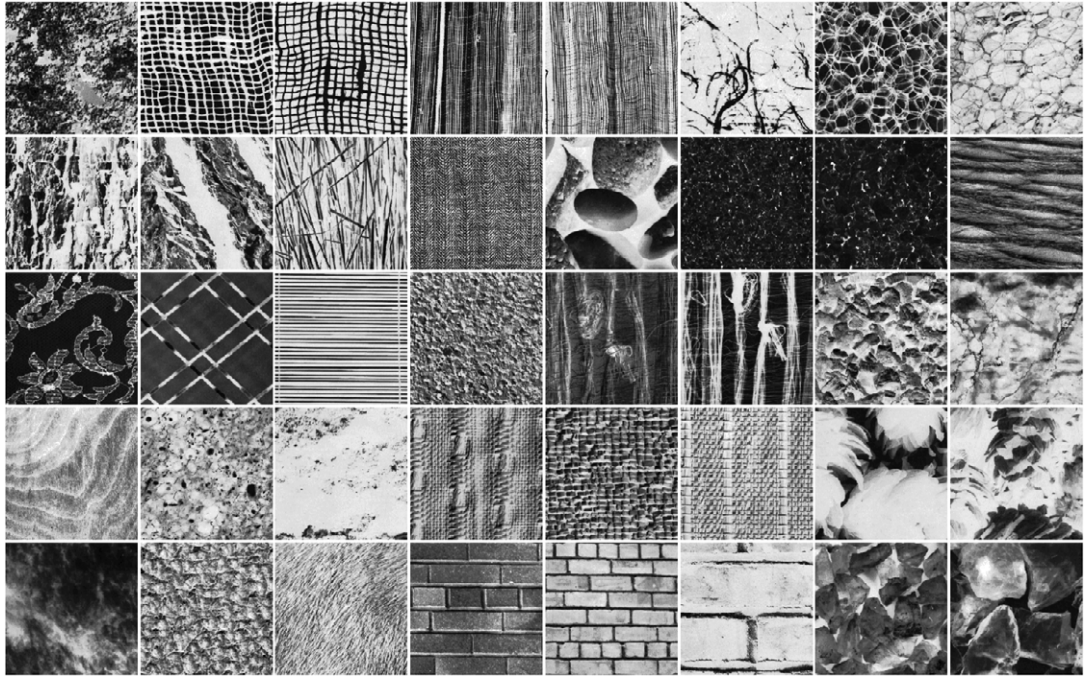

Figure 3. Example of 40 Brodatz texture classes used in the experiment. Each image is 200×200 pixels and has 256 gray levels.
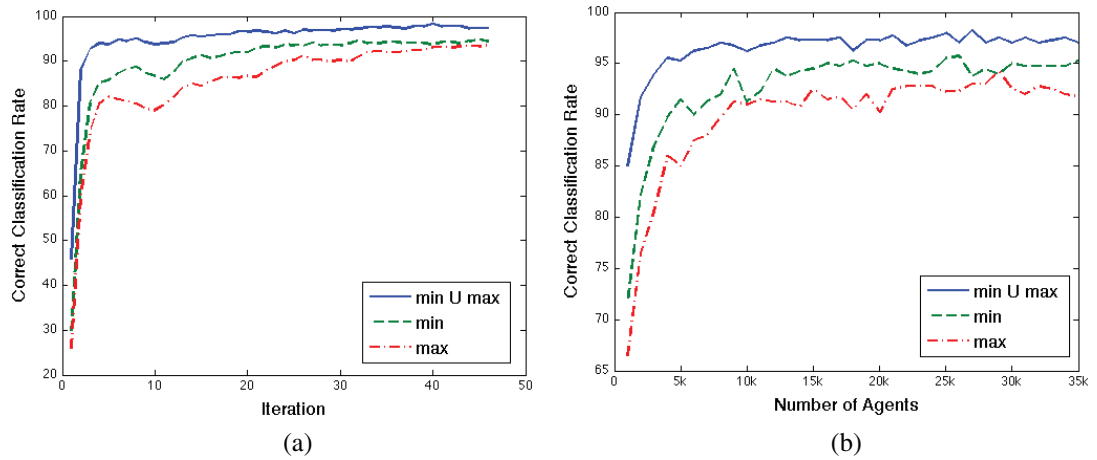

Figure 4. Comparison of artificial crawler methods for different values of (a) iterations and (b) number of agents in the Brodatz dataset.
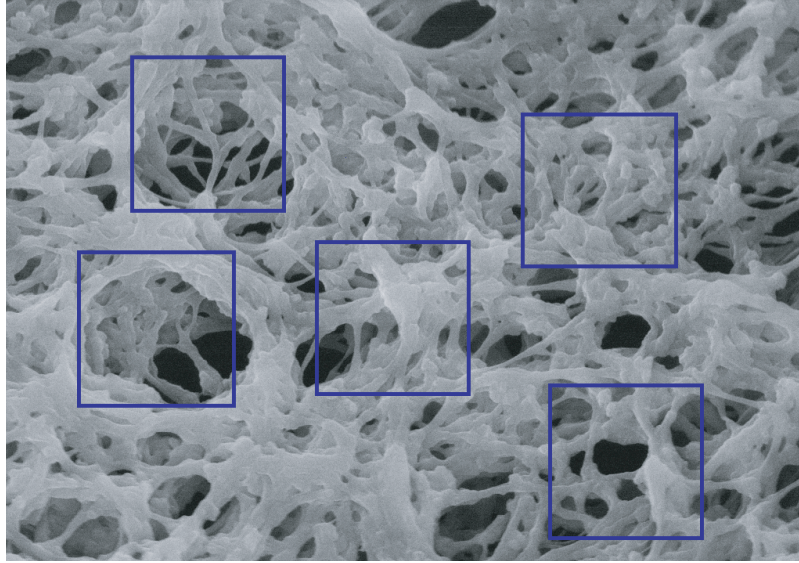
initial energy ϵ of 10 units and the loss for each iteration consumes 1 unit of energy. The absorption rate was set to 0.01 in terms of the current pixel. The survival threshold and the upper bound of energy were set to 1 and 12 units, respectively.

4.2. Performance evaluation

4.2.1. Experiment 1. First, we perform an analysis of our method on the Brodatz dataset. Figure 4(a) presents the correct classification rate versus the number of iterations. The results for the original artificial crawler are shown as curve max while the results for our method are shown as curve min ∪ max. For a complete comparison, we also provide the results for a method where agents move to pixels with a lower intensity—curve min. As can be seen, the proposed method provided the highest correct classification rates for

Table 1. Experimental results for texture methods in the Brodatz dataset.

Method	Images correctly classified	Correct classification (%)
Fourier descriptors [8]	346	86.50 ($\pm$6.58)
Co-occurrence matrices [5]	365	91.25 ($\pm$2.65)
Original artificial crawler [18]	372	93.00 ($\pm$5.50)
Gabor filter [10]	381	95.25 ($\pm$3.43)
Proposed method	393	98.25 ($\pm$1.69)

Figure 5. Samples picked randomly for the glycerol concentration of 2.5%.

all values of iterations. These experimental results indicate that the proposed method significantly improves performance over the traditional methods. We can also observe that the rule min provided higher rates than the rule max, given the idea that valleys are more discriminative than peaks in the Brodatz dataset.

Another important parameter of the artificial crawler method is the number of agents. Figure 4(b) shows the correct classification rates versus the number of agents. As in the previous experiment, our method achieved the highest rates compared to the other two strategies. Again, the rule min provided higher rates than the rule max. Another important observation from figure 4(b) is that using a few agents, the methods achieved good classification results, which makes the artificial crawler method suitable for real time applications. Using these two plots, we can determine the best parameters of our method as $t_{max} = 41$ and $n = 27k$.

The results of the proposed method are compared with existing texture analysis methods in table 1. It is observed that our method outperforms the state-of-the-art method. The highest classification rate of 98.25%($\pm$1.69) was obtained by our method, which is followed by a classification rate of 95.25%($\pm$3.43) obtained by the Gabor filter, one of the most traditional texture analysis methods.

4.2.2. Experiment 2. In this experiment, we present a comparative study of our approach to assess the quality of the silk fibroin scaffolds. Our goal is to provide an effective method to support the visual analysis, thus reducing the subjectiveness of conclusions based on human analysis. The potential of the silk fibroin is enhanced by including glycerol solutions during scaffold formation [17]. In general, such concentrations can range from 0 to 10% with step of 2.5%. This dataset contains five classes, each consisting of ten 200×200 pixel images. Figure 5 shows three samples for each concentration.

We perform the same experiment to determine the best parameters of iteration and number of agents in the silk fibroin dataset. Figure 6(a) presents the evaluation of *t* while figure 6(b) presents the evaluation of *n* for
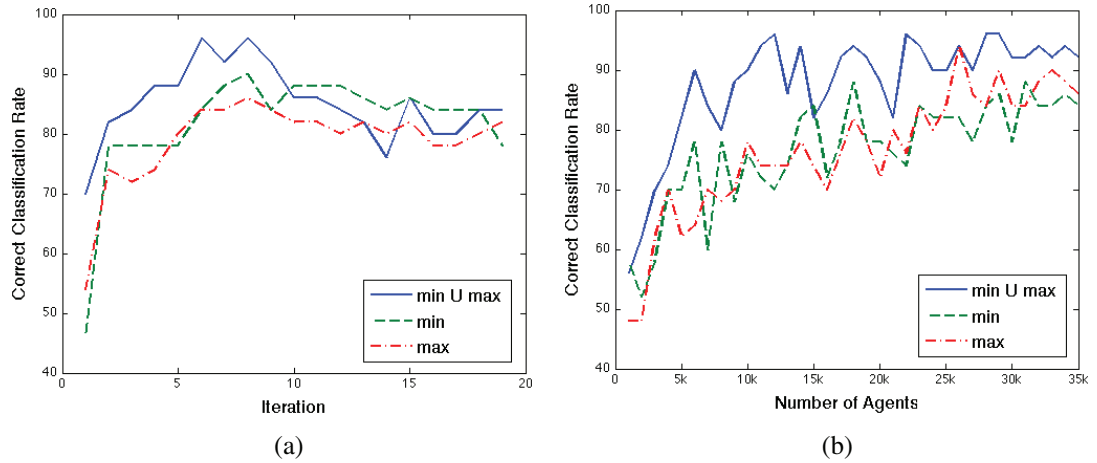
Figure 6. Comparison of artificial crawler methods for different values of (a) iterations and (b) number of agents in the silk fibroin dataset.

Table 2. Experimental results for texture methods in the silk fibroin dataset.

Method	Images correctly classified	Correct classification (%)
Fourier descriptors [8]	39	78.00 ($\pm$22.01)
Co-occurrence matrices [5]	47	94.00 ($\pm$9.66)
Original artificial crawler [18]	42	84.00 ($\pm$15.78)
Gabor filter [10]	31	62.00 ($\pm$19.44)
Proposed method	48	96.00 ($\pm$8.43)

different artificial crawler methods. Using both plots, we found that the best results are achieved for $t_{max} = 7$ and $n = 28k$.

In the silk fibroin dataset, our method achieved the highest classification rates when compared with traditional texture analysis methods. The experimental results, presented in table 2, show that our method achieved a classification rate of 96%($\pm$8.43). These experimental results indicate that our method is consistent and can be applied in real-world situations.

5. Computational complexity

The proposed method initiates n artificial crawlers and each one performs a walk with t_{max} steps. The steps of all artificial crawlers are stated to a complexity of $O(n \times t_{max})$. Once we run the artificial crawlers for both rules, the computational complexity is given by $O(2 \times n \times t_{max})$. For comparison, we have used $(n = 27k, t_{max} = 41)$ and $(n = 28k, t_{max} = 7)$ in the Brodatz and silk fibroin datasets, respectively. We can see that the artificial crawlers need a few steps to achieve the highest correct classification rates.

Although our strategy doubles the computational complexity, experimental results indicate that the proposed method significantly improves the classification rate, e.g. from 93 to 98.25% on the Brodatz dataset and 84 to 96% on the silk fibroin dataset, over the original approach. Furthermore, the proposed method still has a good complexity in comparison to the complexities of well-known methods for texture classification, such as the complexities of Gabor filters ($O((w * h) \log (w * h))$) and co-occurrence matrices ($O(w * h)$), where w and h correspond to the width and height of the image, respectively, and $(w * h)$ is the number of pixels of the image. It should be noted that the number of artificial crawlers is, usually, less than the number of pixels, i.e. $n < (w * h)$. For instance, $n = 27k$ and $(w * h) = 40k$ in the Brodatz dataset.

6. Conclusion

In this paper we presented a novel approach based on the artificial crawler model for texture classification. We have demonstrated how the feature space can be improved by combining *min* and *max* curves, instead of using only the strategy for the maximum intensity of the pixels. Although our approach provides a feature vector with double the dimensionality, the correct classification rate was superior compared with the original approach on the most popular benchmark for texture analysis. Furthermore, we successfully tested our strategy on silk fibroin scaffold analysis. This strategy can be extended to explore different imaging applications. As part of the future work, we plan to focus on evaluating the deterministic sampling, i.e. each pixel of the image is initialized with an agent.

Acknowledgments

References   Q3

[1] Reis M S and Bauer A 2010 Image-based classification of paper surface quality using wavelet texture analysis *Comput. Chem. Eng.* **34** 2014–21
[2] Machado B B, Casanova D, Gonçalves W N and Bruno O M 2013 Partial differential equations and fractal analysis to plant leaf identification *J. Phys.: Conf. Ser.* **410** 012066
[3] Corpetti T and Planchon O 2011 Front detection on satellite images based on wavelet and evidence theory: application to the sea breeze fronts *Remote Sens. Environ.* **115** 306–24
[4] Omar S and Al-Kadi 2010 Texture measures combination for improved meningioma classification of histopathological images *Pattern Recognit.* **43** 2043–53
[5] Haralick R M, Shanmugam K and Dinstein I 1973 Textural features for image classification *IEEE Trans. Syst. Man Cybern.* **3** 610–21
[6] Kashyap R L and Khotanzad A 1986 A model-based method for rotation invariant texture classification *IEEE Trans. Pattern Anal. Mach. Intell.* **8** 472–81
[7] Cross G R and Jain A K 1983 Markov random field texture models *IEEE Trans. Pattern Anal. Mach. Intell.* **5** 25–39
[8] Azencott R, Wang J P and Younes L 1997 Texture classification using windowed Fourier filters *IEEE Trans. Pattern Anal. Mach. Intell.* **19** 148–53
[9] Machado B B, Gonçalves W N and Bruno O M 2011 Enhancing the texture attribute with partial differential equations *ACIVS* pp 337–48
[10] Gabor D 1946 Theory of communication *J. Inst. Electron. Eng.* **93** 429–57   Q4
[11] Daubechies I 1992 *Ten Lectures on Wavelets* (Philadelphia, PA: SIAM)
[12] Bruno O M, de Oliveira Plotze R, Falvo M and de Castro M 2008 Fractal dimension applied to plant identification *Inform. Sci.* **178** 2722–33
[13] Gonçalves W N and Bruno O M 2013 Combining fractal and deterministic walkers for texture analysis and classification *Pattern Recognit.* **46** 2953–68
[14] Backes A R, Gonçalves W N, Martinez A S and Bruno O M 2010 Texture analysis and classification using deterministic tourist walk *Pattern Recognit.* **43** 685–94
[15] Gonçalves W N, Backes A R, Martinez A S and Bruno O M 2012 Texture descriptor based on partially self-avoiding deterministic walker on networks *Expert Syst. Appl.* **39** 11818–29
[16] Altman G, Diaz F, Jakuba C, Calabro T, Horan R, Chen J, Lu H, Richmond J and Kaplan D 2003 Silk-based biomaterials *Biomaterials* **24** 401–16
[17] Shenzhou L, Xiaoqin W, Qiang L, Xiaohui Z, Jonathan A K, Neha U, Omenetto F and Kaplan D L 2010 Insoluble and flexible silk films containing glycerol *Biomacromolecules* **11** 143–50
[18] Zhang D and Chen Y Q 2004 Classifying image texture with artificial crawlers *IAT'04: Int. Conf. on Intelligent Agent Technology* (Los Alamitos, CA: IEEE Computer Society) pp 446–9
[19] Zhang D and Chen Y Q 2005 Artificial life: a new approach to texture classification *Int. J. Pattern Recognit. Artif. Intell.* **19** 355–74

[20] Machado B B, Gonçalves W N and Bruno O M 2013 Material quality assessment of silk nanofibers based on swarm intelligence *J. Phys.: Conf. Ser.* **410** 012163

[21] Brodatz P 1966 *Textures: A Photographic Album for Artists and Designers* (New York: Dover)

[22] Fukunaga K 1990 *Introduction to Statistical Pattern Recognition* 2nd edn (San Diego, CA: Academic)

[23] Fidler S, Skocaj D and Leonardis A 2006 Combining reconstructive and discriminative subspace methods for robust classification and regression by subsampling *IEEE Trans. Pattern Anal. Mach. Intell.* **28** 337–50

QUERY FORM

Journal: CSD

Author: B B Machado *et al*

Title: Artificial crawler model for texture analysis on silk fibroin scaffolds

Article ID: csd 470383

Page 1

Q1.
Author: Do you mean rendering or displaying? Please check.

Page 2

Q2.
Author: Please confirm if edits retain meaning.

Page 9

Q3.
Author: Please check the details for any journal references that do not have a blue link as they may contain some incorrect information. Pale purple links are used for references to arXiv e-prints.

Q4.
Author: Please provide the complete details in ref. [9].